



Review Article

Endoscope-assisted microsurgical retrosigmoid approach to the lateral posterior fossa: Cadaveric model and a review of literature

Mohammed A. Fouda¹, Yasser Jeelani^{2,3}, Abdulkarim Gokoglu², Rajiv R. Iyer¹, Alan R. Cohen¹

¹Division of Pediatric Neurosurgery, Department of Neurosurgery, Johns Hopkins University School of Medicine, Baltimore, Maryland, ²Department of Neurosurgery, Brigham and Woman's Hospital, Boston, Massachusetts, ³Department of Neurosurgery, Boston Children's Hospital, Boston, Massachusetts.

E-mail: *Mohammed A. Fouda - mfouda1@jhmi.edu; Yasser Jeelani - yjeelani@bwh.harvard.edu; Abdulkarim Gokoglu - akerimg@hotmail.com; Rajiv R. Iyer - rri202@gmail.com; Alan R. Cohen - alan.cohen@jhmi.edu



***Corresponding author:**

Mohammed A. Fouda,
Division of Pediatric
Neurosurgery, Department
of Neurosurgery, Johns
Hopkins University School of
Medicine, Baltimore, Maryland,
United States.

mfouda1@jhmi.edu

Received : 13 February 2021

Accepted : 20 July 2021

Published : 16 August 2021

DOI

10.25259/SNI_157_2021

Quick Response Code:



ABSTRACT

Background: The advancement of endoscopic techniques in the past decade has improved the surgical management of cerebellopontine angle (CPA) tumors. Endoscope-assisted microsurgery improves the ability to evaluate the extent of resection, achieve safe tumor resection and reduce the risk of surgery-related morbidity.

Methods: In this study, we used a cadaveric model to demonstrate a step by step endoscope-assisted microsurgery of the retrosigmoid approach to the lateral posterior fossa.

Results: Retrosigmoid craniotomies were performed on four latex-injected cadaver heads (eight CPAs). Microsurgical exposures were performed to identify neurovascular structures in each segment. 0° and 30° rigid endoscope lenses were subsequently introduced into each corridor and views were compared in this manner. The endoscopic images were compared with the standard microscopic views to determine the degree of visualization with each technique. In each case, better visualization was provided by both the 0° and 30° endoscope lenses. Endoscopic views frequently clarified neurovascular relationships in obscured anatomic regions.

Conclusion: Endoscope-assisted microsurgery could allow better visualization of various regions of the posterior fossa. Surgical planning for posterior fossa lesions should include consideration of this combined approach.

Keywords: Cerebellopontine, Endoscope, Posterior fossa, Retrosigmoid, Visualization

INTRODUCTION

The advancement of endoscopic techniques in the past decade has improved the surgical management of cerebellopontine angle (CPA) tumors.^[2,11,23,45] Endoscope-assisted microsurgery improves the ability to evaluate the extent of resection, achieve safe tumor resection, and reduces the risk of surgery-related morbidity.^[2] Endoscope-assisted microsurgery has been well studied and applied for CPA tumors, microvascular decompression (MVD), and aneurysm surgery.^[2,7,18,21,26,33,36,45,47] The endoscope, used as a tool for better surgical visualization.^[2,10,44,45]

The growing experience with neuro-endoscope and improvement of the optical technology has facilitated the ability to achieve gross total resection (GTR) of CPA tumors.^[46] The endoscope

This is an open-access article distributed under the terms of the Creative Commons Attribution-Non Commercial-Share Alike 4.0 License, which allows others to remix, tweak, and build upon the work non-commercially, as long as the author is credited and the new creations are licensed under the identical terms.

©2021 Published by Scientific Scholar on behalf of Surgical Neurology International

permits neurosurgeons to look into spaces outside the microscopic corridor, to look around the surgical corners, and improves illumination and magnification in deep cavities.^[13,41]

In this study, we used a cadaveric model to demonstrate a step by step endoscope-assisted microsurgery of the retrosigmoid approach to the lateral posterior fossa.

MATERIALS AND METHODS

Eight retrosigmoid craniotomies were performed on four colored latex-injected cadaveric head specimens. The head was fixed on a Mayfield head holder and rotated no more than 30° toward the floor, slightly flexed forward, and translated posteriorly. Microsurgical dissection was performed under $\times 3\text{--}\times 24$ magnification (Global Surgical, St. Louis, MO, USA). Endoscopic visualization was obtained with 4 mm 0° and 30° rigid Hopkins' lens systems (Karl Storz, Tuttlingen, Germany).

RESULTS

Positioning

Patient should be positioned in a lateral decubitus with the contralateral arm is positioned below the surgical table with a slight flexion. The head is positioned neutral, parallel to the ground, fixed on a Mayfield head holder. The ipsilateral shoulder is slightly displaced inferiorly, with cushions under contralateral armpit and between the knees. The ipsilateral thigh is flexed and prepared for possible fat and fascia harvest.

Skin incision

Linear incision starts 2 cm behind the external ear at the level of the pinna, running inferiorly in a straight line and ends 1 cm inferior to the mastoid tip.

Craniotomy

The burr hole is placed on the asterion and performed with a regular cranial perforator or a high-speed drill. Craniotomy runs about 3 cm posterior to the burr hole and 4 cm inferiorly, then turning anteriorly just parallel to the burr hole. Anteriorly, the remaining anterior cut is performed with the drill. The sigmoid and transverse sinuses must be exposed using the drill.

Superior neurovascular complex

The superior compartment of the posterior fossa is contiguous with the undersurface of the tentorium cerebelli and extends inferiorly to the level of the mid-pons where

the cisternal segment of the trigeminal nerve exits the brainstem.

Using the microscope, and on inferomedial retraction of the cerebellum, the superior petrosal vein (SPV) is visible, obscuring part of the trigeminal nerve along its course from the pons (origin) to Meckel's cave (entry). The superior cerebellar artery (SCA) was seen within the ambient cistern lateral to the brainstem. Moving downwards, the SCA was lost to the microscopic view as it coursed along the dorsal aspect of the midbrain toward the tentorial surface. The trochlear nerve was seen superior to the SCA, running along the cerebellomesencephalic fissure [Figure 1a and b]. The SCA bifurcated at the level of the cerebellomesencephalic fissure with the trochlear nerve weaving among the two branches. The trigeminal nerve was not properly visualized microscopically due to the presence of the SCA superiorly and the anterior inferior cerebellar artery (AICA) inferiorly.

Using the endoscope (0° lens), the SPV was perfectly seen in conjunction with the dorsal surface of the trigeminal nerve [Figure 1c]. Laterally, the trochlear nerve curved around the side of the brainstem under the tentorial edge. The proximal

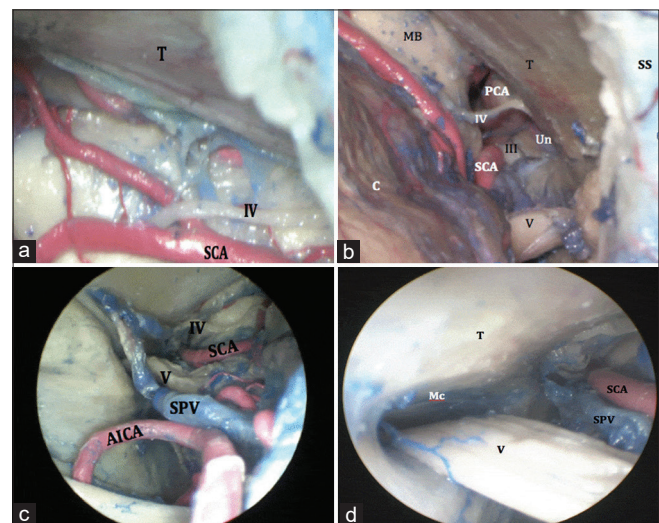


Figure 1: (a) Microscopic view of the superior lateral posterior fossa. The trochlear nerve is superior to the SCA. (b) Microscopic view of the superior lateral posterior fossa, showing the contents of the ambient cistern. The trochlear nerve can be seen between the PCA superiorly and the SCA inferiorly. The oculomotor nerve (III) can be also seen traveling in the interpeduncular cistern while coursing medially in relation to the Un. A small segment of the trigeminal nerve (V) is also visualized. (c) Endoscopic view (0° lens) of the superior lateral posterior fossa above. The trigeminal nerve lies posterior to the SPV. (d) Endoscopic view (30° lens) of the superior lateral posterior fossa, aiming laterally in order to show the trigeminal nerve traveling into Mc. AICA: Anterior inferior cerebellar artery, SPV: Superior petrosal vein, SCA: Superior cerebellar artery, Mc: Meckel's cave, Un: uncus, PCA: Posterior cerebral artery.

SCA and the posterior cerebral artery (PCA) were seen where they emerge from the ambient cistern. Medially, the trochlear nerve and the SCA were seen in the cerebellomesencephalic fissure, all the way proximal to the origin of the trochlear nerve on the dorsal aspect of the brainstem, close to midline.

Using the endoscope (30° lens), the porus trigeminus, which was mostly obscured under microscopic view due to the presence of the suprameatal tubercle, was nicely seen [Figure 1d]. Medially, the endoscope also provided a clear view of the trigeminal root entry zone at the level of the midpons. Anteriorly, the trochlear nerve was seen as it courses toward the tentorium. Moving forward across the ambient cistern, the origin of the ipsilateral oculomotor nerve arising within the interpeduncular fossa could be visualized, in addition to the bifurcation of the basilar artery.

Middle neurovascular complex

Using the microscope, the AICA was seen on the lateral surface of the pons, superior to the inferior olive. It is contiguous with the facial-vestibulocochlear nerve complex before its course along the lateral cerebellar surface [Figure 2a]. The labyrinthine artery and other branches off the AICA were seen accompanying the facial-vestibulocochlear nerve complex as it enters the internal auditory canal (IAC). The junction of the facial-vestibulocochlear nerve complex with the brainstem was obscured under the microscopic vision by the flocculus. Gentle medial retraction of the flocculus revealed the foramen of Luschka, over the lateral recess of the fourth ventricle. The proximal cisternal segment of the facial nerve was hidden anterior to the vestibulocochlear nerve at its origin, although its junction with the brainstem is slightly more superior to that of the vestibulocochlear nerve. Only a small portion of the internal acoustic meatus was seen due to presence of the bony ridge overlying the porus acusticus. The abducens nerve was partially seen as it emerges from the brainstem anteromedial to the vestibulocochlear nerve.

Using the endoscope (0° lens), superomedial retraction of the flocculus was required to visualize the junction of the facial-vestibulocochlear nerve complex with the brainstem. The meatal opening was more clearly visualized, in addition to the labyrinthine and subarcuate arteries [Figure 2b]. The AICA and its relationship with the facial-vestibulocochlear nerve complex were perfectly seen and inspected [Figure 2b]. Advancing the endoscope beyond the plane of the facial-vestibulocochlear nerve complex brought the abducens nerve into vision. However, this particular trajectory over the vestibulocochlear nerve did not permit lateral visualization of the abducens nerve as it exits the posterior fossa by piercing the dura into the Dorello's canal.

Using the endoscope (30° lens) allowed a proper inspection of the internal acoustic meatus and the distal portions of

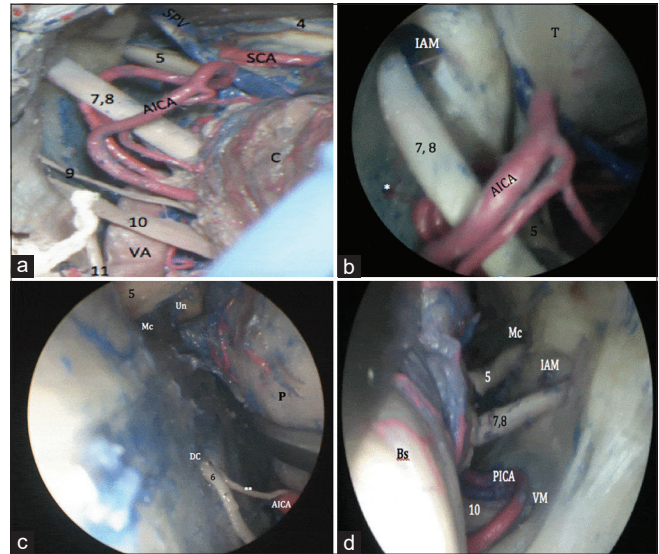


Figure 2: (a) Microscopic view of the middle lateral posterior fossa. The facial-vestibulocochlear nerve complex is seen in relation to the caudal loop of the AICA. (b) Endoscopic view (0° lens) of the middle posterior fossa. The meatal opening was more clearly visualized, in addition to the labyrinthine artery. The facial-vestibulocochlear nerve complex is seen in relation to the caudal loop of the AICA. The trigeminal nerve (V) was partially obscured by the superior petrosal vein. (c) Microscopic view (30° lens) angled endoscopic view of the middle lateral posterior fossa. The exit of the abducens nerve (6) into DC is well visualized. (d) Microscopic view (30° lens) angled endoscopic view of the middle lateral posterior fossa allowed good visualization of the V, VII, VIII, and X as they entered their respective skull base foramina. AICA: Anterior inferior cerebellar artery, PICA: Posterior inferior cerebellar artery, DC: Dorello's canal, VA: Vertebral artery, SPV: Superior petrosal vein, SCA: Superior cerebellar artery, Mc: Meckel's cave, Un: uncus.

the facial-vestibulocochlear nerve complex. It also allowed better visualization of the origin of the facial nerve as it courses anterior and parallel to the vestibulocochlear nerve. Medially, the inferior olive could be inspected, as well as the terminal branches of the AICA. The entry of the abducens nerve into Dorello's canal could be visualized anterior to the plane of the facial-vestibulocochlear nerve complex at the level of the pontomedullary junction [Figure 2c]. Advancing the endoscope inferior to the plane of the facial-vestibulocochlear nerve complex, allowed good visualization of the V, VII, VIII, IX, and X as they entered their respective skull base foramina [Figure 2d].

Inferior neurovascular complex

Using the microscope, the dorsal surface of the glossopharyngeal and vagus nerves was seen posterior to the inferior olive. The junction of the IX and X cranial nerves with the brainstem was visualized with a slight superomedial retraction of the cerebellum. The glossopharyngeal nerve

was seen arising below the pontomedullary junction, on the dorsal aspect of the olivary body. The proximal vagus nerve was partially obscured by the presence of the lateral recess of the fourth ventricle and part of the choroid plexus through the foramen of Luschka [Figure 3a]. The vagal nerve rootlets coalesced in the cerebellomedullary cistern inferior to the glossopharyngeal nerve. The jugular foramen could not be entirely visualized with the microscope alone. The posterior inferior cerebellar artery (PICA) was identified at its origin from the vertebral artery [Figure 3b]. The PICA weaves around the hypoglossal rootlets before curling around onto the cerebellar tonsils through a series of craniocaudally-oriented loops. The hypoglossal nerve travels anteriorly at the olivo medullary junction, inferior to the origin of the IX and X cranial nerves in the pre olivary sulcus [Figure 3b]. The hypoglossal canal (HC) was not visualized under the microscope. The accessory nerve was also seen at the level of the lower half of the inferior olive.

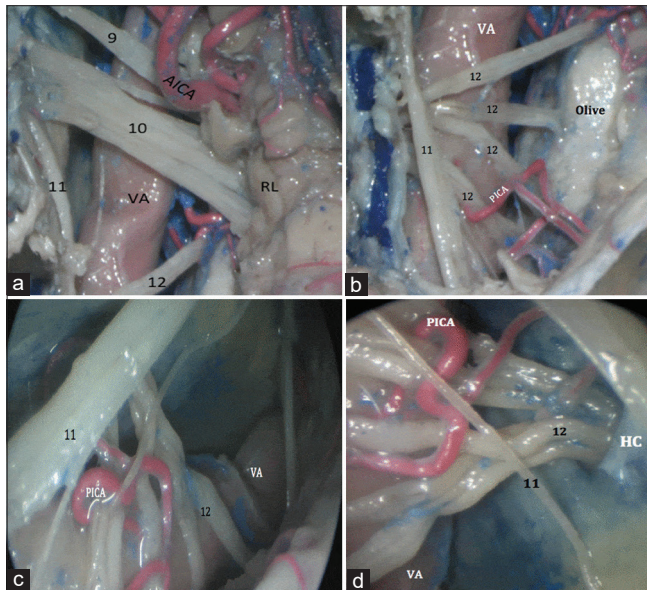


Figure 3: (a) Microscopic view of the inferior lateral posterior fossa showing the IX, X and XI cranial nerves (9, 10, 11) running over the dorsal surface of the VA. The proximal vagus nerve was partially obscured by the presence of the lateral recess of the fourth ventricle. A caudal loop of the AICA is seen in close relation to the IX cranial nerve. (b) Microscopic view of the inferior lateral posterior fossa, showing the origin of the hypoglossal nerve (12) from the olivary groove on the brainstem. The origin of PICA from the dorsal surface of the VA and its course through several hypoglossal rootlets to finally to reach the cerebellar tonsils. (c) Endoscopic view (0° lens) of the inferior lateral posterior fossa, showing the distal XII cranial nerve (12). The HC is obscured by the XI cranial nerve (11). (d) Endoscopic view (30° lens) of the inferior lateral posterior fossa, showing aimed laterally showing the exit of the XII cranial nerve (12) through the HC. VA: Vertebral artery, AICA: Anterior inferior cerebellar artery, PICA: Posterior inferior cerebellar artery, HC: Hypoglossal canal.

Using the endoscope (0° lens) provided better views of the dorsal surfaces of the glossopharyngeal and the vagal nerves. Advancing the endoscope beyond the plate of IX and X cranial nerves, the rootlets of the hypoglossal nerve could be inspected [Figure 3c]. However, the foramina for the lower cranial nerves were unable to be visualized.

Using the endoscope (30° lens) allowed excellent visualization the PICA, rootlets of the lower cranial nerves, and the bony exits of cranial nerves IX, X, and XII. Medial exploration allowed for inspection of the rhomboid lip and the origins of the glossopharyngeal, vagal, and hypoglossal nerves, as well as the foramen of Luschka. Peering laterally, the jugular foramen could be visualized along with the intervening dural septum lying between the exits of the two nerves. The accessory nerve was also seen entering the jugular foramen after coalescence of its various rootlets and ascension along the lateral border of the medulla, inferior to the olive. The HC was perfectly visualized as well [Figure 3d].

DISCUSSION

In this study, we showed the endoscope-assisted microsurgical anatomy of the retrosigmoid approach. In the superior neurovascular complex, the endoscope allowed us to nicely visualize the SPV, the trochlear, the proximal SCA and the PCA, the porus trigeminus, the trigeminal root entry zone at the level of the mid-pons and the origin of the ipsilateral oculomotor nerve arising within the interpeduncular fossa, in addition to the bifurcation of the basilar artery. Also in the middle neurovascular complex, the endoscope allowed us to visualize the junction of the facial-vestibulocochlear nerve complex with the brainstem, the meatal opening, the labyrinthine and subarcuate arteries, the AICA and its relationship with the facial-vestibulocochlear nerve complex, the abducens nerve, the origin of the facial nerve as it courses anterior and parallel to the vestibulocochlear nerve, the inferior olive and the terminal branches of the AICA in addition to the V, VII, VIII, IX, and X as they entered their respective skull base foramina. Meanwhile, in the inferior neurovascular complex, the endoscope was an asset to visualize the dorsal surfaces of the glossopharyngeal and the vagal nerves, the rootlets of the hypoglossal nerve, the PICA, rootlets of the lower cranial nerves, and the bony exits of cranial nerves IX, X, and XII.

In 1917, Doyen and Spencer-Browne was the first to describe a unique endoscopic sectioning of the trigeminal nerve as a cure for trigeminal neuralgia.^[12,30] In 1970s, several reports have shown the growing utilization of endoscopy in the CPA surgery.^[3,17,35,38] In 1990s, endoscope-assisted microsurgery has been utilized for the management of tumors of the IAC, hemifacial spasm, and trigeminal neuralgia.^[29,30,32,34] The endoscope has conferred the ability to look around the corners with least risk of brain retraction.^[4,9,22,24]

In 1977, Jannetta *et al.* described the principles of MVD. However, this procedure was associated with a risk of failure, recurrence, and neurological deficits.^[5,8,16,19,20,25,27,39,42] The desire for safe minimally invasive approaches to the posterior fossa has led to the application of endoscopic techniques for nerve decompression from compressing vasculature.^[6] Visualization of the entire cisternal facial nerve segment, often obstructed by both the flocculus and choroid plexus emanating from the foramen of Luschka, is possible with the use of endoscopes.^[14,43] The key factors for a successful MVD surgery include a precise visualization of all the nerve-vessel conflicts and a confirmation of a proper nerve decompression by the end of the procedure.^[39] Given the anatomy of the posterior fossa and the limited size of the craniotomy, adequate visualization of the full course of the facial nerve and the porus portion, is difficult and challenging by the utilization of the surgical microscope only.^[19,20,25,39] To overcome such limitations, endoscope-assisted microscopic surgery was introduced to properly identify the site of the neurovascular compression and reduce the risk of complications.^[1,4,15,24,28,30,34,39] Endoscope-assisted MVD of the facial nerve demonstrated an additional 72 % accuracy rate in identifying the nerve-vessel conflicts without dislocation of the acoustic-facial bundle and significant cerebellar retraction, resulting in a lower risk of neurological deficits.^[4,15,24,28,30]

Corrivetti *et al.* reported that after microsurgical resection of vestibular schwannoma in 32 patients, the endoscopic inspection showed residual tumor in the lateral portion of the IAC in all cases. Therefore, they were able to accomplish GTR in the majority of cases and near total resection in those cases in which a thin layer of tumor capsule was left around the facial nerve because of firm adherences of the tumor capsule.^[11] Hearing preservation also implies anatomical respect of the inner ear structures when exposing the fundus of the IAC. The most lateral part of the IAC is not sufficiently visualized under microscopic view only. Mazzoni *et al.* described the microsurgical technique of retrolabyrinthine meatotomy that allows a safe exposure of the fund of the IAC by a careful drilling of the IAC all the way to the fundus.^[31] Pillai *et al.* described a unique endoscope-assisted microsurgical technique on a cadaveric model, achieving an excellent exposure of the fallopian portion of the fundus of the ICA.^[37] Endoscopic assistance may confer the surgeon to decrease the amount of bone drilled in the posterior wall of the IAC, reducing the risk of labyrinth injuries.^[2,40] Abolfotoh *et al.* described, in a surgical series of 50 CPA tumors, the presence of additional tumor in 64% of the cases in which the sole microscopic resection was believed to be GTR, demonstrating that endoscopic assistance had a relevant role in obtaining a GTR.^[2]

CONCLUSION

Endoscope-assisted microsurgery could allow better visualization of superior the various regions of the posterior fossa. The use of straight and angled endoscope lenses allows for excellent visualization of areas obscured from the microscopic vision, including but not limited to the trigeminal porus, internal acoustic meatus, cranial nerve root entry zones, as well as important neurovascular anatomic relationships. Surgical planning for posterior fossa lesions should include consideration of this combined approach.

Declaration of patient consent

Patient's consent not required as there are no patients in this study.

Financial support and sponsorship

Nil.

Conflicts of interest

There are no conflicts of interest.

REFERENCES

1. Abdeen K, Kato Y, Kiya N, Yoshida K, Kanno T. Neuroendoscopy in microvascular decompression for trigeminal neuralgia and hemifacial spasm. *Neurol Res* 2000;22:522-6.
2. Abolfotoh M, Bi WL, Hong CK, Almefty KK, Boskovitz A, Dunn IF, *et al.* The combined microscopic-endoscopic technique for radical resection of cerebellopontine angle tumors. *J Neurosurg* 2015;123:1301-11.
3. Apuzzo ML, Heifetz MD, Weiss MH, Kurze T. Neurosurgical endoscopy using the side-viewing telescope. *J Neurosurg* 1977;46:398-400.
4. Badr-El-Dine M, El-Garem H, Talaat A, Magnan J. Endoscopically assisted minimally invasive microvascular decompression of hemifacial spasm. *Otol Neurotol* 2002;23:122-8.
5. Barker FG, Jannetta PJ, Bissonette DJ, Shields PT, Larkins MV, Jho HD. Microvascular decompression for hemifacial spasm. *J Neurosurg* 1995;82:201-10.
6. Bohman L-E, Pierce J, Stephen JH, Sandhu S, Lee JY. Fully endoscopic microvascular decompression for trigeminal neuralgia: Technique review and early outcomes. *Neurosurg Focus* 2014;37:E18.
7. Broggi M, Acerbi F, Ferroli P, Tringali G, Schiariti M, Broggi G. Microvascular decompression for neurovascular conflicts in the cerebello-pontine angle: Which role for endoscopy? *Acta Neurochir (Wien)* 2013;155:1709-16.
8. Campero A, Herreros I, Barrenechea I, Andjel G, Ajler P, Rhoton A. Microvascular decompression in hemifacial spasm: 13 cases report and review of the literature. *Surg Neurol Int*

- 2016;7 Suppl 8:S201-7.
9. Charalampaki P, Kafadar A, Grunert P, Ayyad A, Perneczky A. Vascular decompression of trigeminal and facial nerves in the posterior fossa under endoscope-assisted keyhole conditions. *Skull Base* 2008;18:117-28.
 10. Chovanec M, Zvěřina E, Profant O, Skřivan J, Čákrť O, Lisý J, *et al.* Impact of video-endoscopy on the results of retrosigmoid-transmeatal microsurgery of vestibular schwannoma: Prospective study. *Eur Arch Otorhinolaryngol* 2013;270:1277-84.
 11. Corrivetti F, Cacciotti G, Scavo CG, Roperto R, Stati G, Sufianov A, *et al.* Flexible endoscopic assistance in the surgical management of vestibular schwannomas. *Neurosurg Rev* 2021;44:363-71.
 12. Doyen EL. *Surgical Therapeutics and Operative Technique*. United Kingdom: William Wood; 1917.
 13. Ebner F, Roser F, Thaher F, Schittenhelm J, Tatagiba M. Balancing the shortcomings of microscope and endoscope: Endoscope-assisted technique in microsurgical removal of recurrent epidermoid cysts in the posterior fossa. *Minim Invasive Neurosurg* 2010;53:218-22.
 14. Eby JB, Cha ST, Shahinian HK. Fully endoscopic vascular decompression of the facial nerve for hemifacial spasm. *Skull Base* 2001;11:189-97.
 15. El-Garem H, Badr-El-Dine M, Talaat A, Magnan J. Endoscopy as a tool in minimally invasive trigeminal neuralgia surgery. *Otol Neurotol* 2002;23:132-5.
 16. Feng BH, Zheng XS, Wang XH, Ying TT, Yang M, Tang YD, *et al.* Management of vessels passing through the facial nerve in the treatment of hemifacial spasm. *Acta Neurochir (Wien)* 2015;157:1935-40.
 17. Fukushima T. Endoscopy of Meckel's cave, cisterna magna, and cerebellopontine angle. *J Neurosurg* 1978;48:302-6.
 18. Gerganov V, Giordano M, Herold C, Samii A, Samii M. An electrophysiological study on the safety of the endoscope-assisted microsurgical removal of vestibular schwannomas. *Eur J Surg Oncol* 2010;36:422-7.
 19. Hanakita J, Kondo A. Serious complications of microvascular decompression operations for trigeminal neuralgia and hemifacial spasm. *Neurosurgery* 1988;22:248-352.
 20. Jannetta PJ, Abbasy M, Maroon JC, Ramos FM, Albin MS. Etiology and definitive microsurgical treatment of hemifacial spasm: Operative techniques and results in 47 patients. *J Neurosurg* 1977;47:321-8.
 21. Jarrahy R, Berci G, Shahinian HK. Endoscope-assisted microvascular decompression of the trigeminal nerve. *Otolaryngol Head Neck Surg* 2000;123:218-23.
 22. Kabil M, Eby J, Shahinian H. Endoscopic vascular decompression versus microvascular decompression of the trigeminal nerve. *Minim Invasive Neurosurg* 2005;48:207-12.
 23. Kawamata T, Kamikawa S, Iseki H, Hori T. Flexible endoscope-assisted endonasal transsphenoidal surgery for pituitary tumors. *Minim Invasive Neurosurg* 2002;45:208-10.
 24. King WA, Wackym PA, Sen C, Meyer GA, Shiau J, Deutsch H. Adjunctive use of endoscopy during posterior fossa surgery to treat cranial neuropathies. *Neurosurgery* 2001;49:108-16.
 25. Kureshi SA, Wilkins RH. Posterior fossa reexploration for persistent or recurrent trigeminal neuralgia or hemifacial spasm: Surgical findings and therapeutic implications. *Neurosurgery* 1998;43:1111-6.
 26. Kurucz P, Baksa G, Patonay L, Thaher F, Buchfelder M, Ganslandt O. Endoscopic approach-routes in the posterior fossa cisterns through the retrosigmoid keyhole craniotomy: An anatomical study. *Neurosurg Rev* 2017;40:427-48.
 27. Liu J, Yuan Y, Fang Y, Zhang L, Xu XL, Liu HJ, *et al.* Microvascular decompression for atypical hemifacial spasm: Lessons learned from a retrospective study of 12 cases. *J Neurosurg* 2016;124:397-402.
 28. Magnan J, Caces F, Locatelli P, Chays A. Hemifacial spasm: Endoscopic vascular decompression. *Otolaryngol Head Neck Surg* 1997;117:308-14.
 29. Magnan J, Chays A, Cohen J, Caces F, Locatelli P. Endoscopy of the cerebellopontine angle. *Rev Laryngol Otol Rhinol (Bord)* 1995;116:115-8.
 30. Magnan J, Chays A, Lepetre C, Pencroffi E, Locatelli P. Surgical perspectives of endoscopy of the cerebellopontine angle. *Otol Neurotol* 1994;15:366-70.
 31. Mazzoni A, Zanoletti E, Denaro L, Martini A, d'Avella D. Retrolabyrinthine meatotomy as part of retrosigmoid approach to expose the whole internal auditory canal: Rationale, technique, and outcome in hearing preservation surgery for vestibular schwannoma. *Oper Neurosurg (Hagerstown)* 2018;14:36-44.
 32. McKennan KX. Endoscopy of the internal auditory canal during hearing conservation acoustic tumor surgery. *Am J Otol* 1993;14:259-62.
 33. Nishiyama Y, Kinouchi H, Horikoshi T. Surgery on intracranial aneurysms under simultaneous microscopic and endoscopic monitoring. *Neurosurgery* 2011;58:84-92.
 34. O'Donoghue GM, O'Tlynn P. Endoscopic anatomy of the cerebellopontine angle. *Otol Neurotol* 1993;14:122-5.
 35. Oppel F, Mulch G. Selective trigeminal root section via an endoscopic transpyramidal retrolabyrinthine approach. *Acta Neurochir Suppl (Wien)* 1979;28:565-71.
 36. Peris-Celda M, da Roz L, Monroy-Sosa A, Morishita T, Rhoton AL Jr. Surgical anatomy of endoscope-assisted approaches to common aneurysm sites. *Neurosurgery* 2014;10:121-44; discussion 144.
 37. Pillai P, Sammet S, Ammirati M. Image-guided, endoscopic-assisted drilling and exposure of the whole length of the internal auditory canal and its fundus with preservation of the integrity of the labyrinth using a retrosigmoid approach: A laboratory investigation. *Neurosurgery* 2009;65 Suppl 6: 53-9; discussion 59.
 38. Prott W. Cisternography of the cerebellopontine angle (author's transl). *HNO* 1974;22:337-41.
 39. Ricci G, Stadio AD, D'Ascanio L, Penna RL, Tralbalzini F, Della Volpe A, *et al.* Endoscope-assisted retrosigmoid approach in hemifacial spasm: Our experience. *Braz J Otorhinolaryngol* 2019;85:465-72.
 40. Samii M, Gerganov V, Samii A. Improved preservation of hearing and facial nerve function in vestibular schwannoma surgery via the retrosigmoid approach in a series of 200 patients. *J Neurosurg* 2006;105:527-35.
 41. Schroeder HW, Oertel J, Gaab MR. Endoscope-assisted microsurgical resection of epidermoid tumors of the cerebellopontine angle. *J Neurosurg* 2004;101:227-32.

42. Sharma R, Garg K, Agarwal S, Agarwal D, Chandra PS, Kale SS, *et al.* Microvascular decompression for hemifacial spasm: A systematic review of vascular pathology, long term treatment efficacy and safety. *Neurol India* 2017;65:493-505.
43. Takemura Y, Inoue T, Morishita T, Rhoton AL Jr. Comparison of microscopic and endoscopic approaches to the cerebellopontine angle. *World Neurosurg* 2014;82:427-41.
44. Tatagiba M, Matthies C, Samii M. Microendoscopy of the internal auditory canal in vestibular schwannoma surgery. *Neurosurgery* 1996;38:737-40.
45. Tatagiba MS, Roser F, Hirt B, Ebner FH. The retrosigmoid endoscopic approach for cerebellopontine-angle tumors and microvascular decompression. *World Neurosurg* 2014;82 Suppl 6:S171-6.
46. Tuchman A, Platt A, Winer J, Pham M, Giannotta S, Zada G. Endoscopic-assisted resection of intracranial epidermoid tumors. *World Neurosurg* 2014;82:450-4.
47. Vickers NJ. Animal communication: When I'm calling you, will you answer too? *Curr Biol* 2017;27:R713-5.

How to cite this article: Fouda MA, Jeelani Y, Gokoglu A, Iyer RR, Cohen AR. Endoscope-assisted microsurgical retrosigmoid approach to the lateral posterior fossa: Cadaveric model and a review of literature. *Surg Neurol Int* 2021;12:416.